第44卷第2期 中国科学技术大学学报 Vol. 44, No. 2
2014年2月 JOURNAL OF UNIVERSITY OF SCIENCE AND TECHNOLOGY OF CHINA Feb. 2014

Article ID: 0253-2778(2014)02-0106-06

Vapor-phase synthesis of single-crystalline Ag nanowires and their SERS properties

LI Zhi, ZHU Wei, YU Qingxuan, YANG Qianhui, SHAO Zhibin, LOU Liren

(*Hefei National Laboratory for Physical Sciences at Microscale, and Department of Physics, University of Science and Technology of China, Hefei* 230026, *China*)

Abstract: Single-crystalline Ag nanowires with a face-centered cubic (fcc) crystal structure were synthesized inside Ag/ZnO coaxial nanocables by the vapor-liquid-solid (VLS) mechanism through a thermal evaporation route. The confinement of the ZnO shell was believed to be responsible for the emergence of the single-crystalline phase. Ag nanowires with different diameters could be obtained by etching Ag/ZnO coaxial nanocables with modulated core-shell ratio determined by Ag concentration in the source. These high-quality silver nanowires were explored as sensitive substrates of surface enhanced Raman scattering (SERS).

Key words: Ag nanowires; chemical vapor deposition (CVD); ZnO; coaxial nanocable; sueface enhanced Raman scattering (SERS)

CLC number: O469 **Document code**: A doi: 10.3969/j.issn.0253-2778.2014.02.005

Citation: Li Zhi, Zhu Wei, Yu Qingxuan, et al. Vapor-phase synthesis of single-crystalline Ag nanowires and their SERS properties[J]. Journal of University of Science and Technology of China, 2014, 44(2): 106-111.

银单晶纳米线的气相合成及其表面增强拉曼散射特性

李 志, 祝 巍, 余庆选, 杨乾辉, 邵智斌, 楼立人

(中国科学技术大学物理系, 合肥微尺度物质科学国家实验室, 安徽合肥 230026)

摘要: 通过气-液-固(VLS)机制, 利用热蒸发方法在Ag/ZnO同轴结构纳米线中合成了单晶Ag纳米线. ZnO壳的限制作用被认为是促成了Ag单晶相的形成. 通过腐蚀掉ZnO壳而获得的银纳米线, 其直径可以通过改变源中银的含量来调控. 这些高质量的银纳米线具有明显的表面增强拉曼散射(SERS)增强效果.

关键词: 银纳米线; 化学气相沉积(CVD); 氧化锌; 同轴结构纳米线; 表面增强拉曼散射(SERS)

Received: 2013-04-02; **Revised**: 2014-01-16

Foundation item: Supported by the National Natural Science Foundation of China (50772110, 50721091), and Fundamental Research Funds for the Central Universities (WK2030000004).

Biography: LI Zhi, male, born in 1982, PhD candidate. Research filed: synthesis and application of nanomaterials. E-mail: lizhi82@mail.ustc.edu.cn

Corresponding author: ZHU Wei, PhD/lecturer. E-mail: zhuw@ustc.edu.cn

0 Introduction

Metal nanostructures have attracted particular attention due to their superior properties and potential applications in catalysis[1-2], optoelectronics[3-4], and optical sensing[5-8]. Notably, surface-enhanced Raman scattering (SERS), which allows the detection of single molecules, is one of the most interesting features of these metal nanostructures[9-13]. Among all metals, silver has the highest electrical and thermal conductivity and also shows the most effective SERS performance in the visible region. A number of chemical approaches have been actively explored to process silver into 1D nanostructures[14-16]. However, most reported methods for the synthesis of Ag nanostructures are wet chemical routes involving the use of surfactants[17-19], templates[20-21], or capping agents.[22-23] Although good control over nanostructure dimensions can be realized in these syntheses, severe post-treatments are required to remove the templates, surfactants, or capping agents from the nanostructure surface, which affects the purity of the materials.

Recently, in order to provide a reliable SERS detection, vapor deposition methods have been developed to prepare silver nanowires with a clean surface, using sources such as Ag_2O or pure Ag[24-25]. The growth process of Ag nanowires by using these vapor deposition methods are all attributed to the vapor-solid (VS) growth mechanism. However, these methods for synthesis of Ag nanowires suffer from several problems, such as low yields, and inability in controlling the diameters of the nanowires.

Herein, we describe a facile two-step thermal evaporation route to fabricate high-yield Ag nanowires via the vapor-liquid-solid (VLS) growth mechanism. The resulting Ag nanowires are single-crystalline and have a face-centered cubic (fcc) structure. Their diameters can be modulated by changing the ratio of Ag in the source. The optical and SERS properties of the resulting Ag nanowires were investigated. The approach we demonstrated here may be extended to synthesize other metal nanowires.

1 Experimental

The Ag nanowires were fabricated by a two-step process. First, Ag/ZnO nanocables were synthesized in a conventional tube furnace as reported previously[26]. Subsequently, Ag nanowires were successfully obtained by etching ZnO shell with 3 mol/L hydrochloric acid solution for 120 min.

The as-prepared Ag nanowires were characterized by field emission scanning electron microscopy (FE-SEM, JEOL JSM-6700F), high-resolution transmission electron microscopy (HRTEM, JEOL model 2010), and X-ray diffraction microscopy (XRD) with Cu K_α radiation (wavelength, 1.504 5 Å).

For preparation of SERS substrates, the synthesized Ag nanowires on the Si substrates were washed with deionized water and then ethanol and dried in air. Then the substrates were immersed in 1 nmol/L aqueous solution of rhodamine B for 30 min, rinsed with deionized water after removal from the solution, and finally dried in air. The Raman instrument used in this study was in confocal configuration (LABRAM-HR) and excited by an Ar laser (514 nm). The spot size of the laser beam on the sample was about 2 μm. The acquisition time of the scattering signal was 1 s.

2 Results and discussion

It has been confirmed that the products of the first step process are nanocables which are made up of ZnO nanotubes filled with silver nanowires in our previous work[26]. A detailed schematic illustration of the formation process is shown in Fig. 1. The formation of the Ag/ZnO nanocables synthesized here can be attributed to the VLS growth mechanism. Briefly, Ag vapor generated

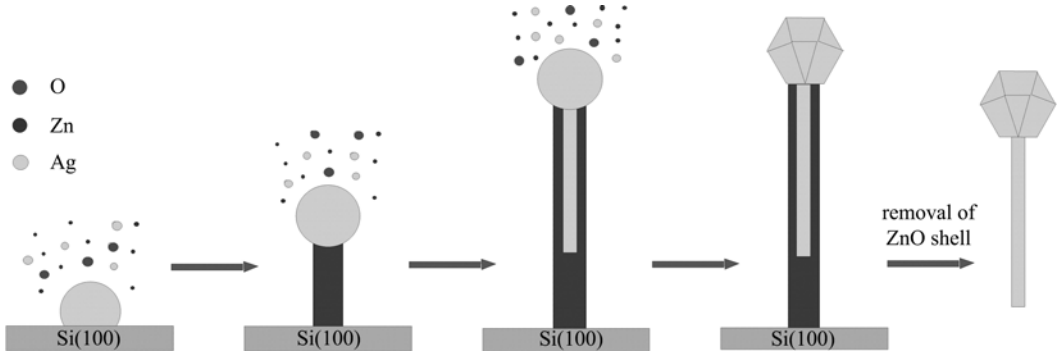

Fig. 1 The schematic illustration of the growth model for Ag nanowires

from the decomposition of $AgNO_3$ is transported and Ag droplets form on the substrate. At the same time, Zn and O vapors are adsorbed on the surface of the Ag droplets which serv as the catalyst, resulting in the growth of ZnO nanowires. With O content decreasing in the droplet, ZnO nanotubes start to form, and the liquid droplet is sucked into the hollow cavity due to the capillarity effect. Zn atoms diffuse out from the alloy and are oxidized to ZnO, leaving Ag to fill the nanotube.

After etching, the final products were obtained. The representative SEM image of the as-obtained samples, as shown in Fig. 2(a), reveals high density of nanowires with a length of tens of micrometers on the Si substrate. The inset is a high-resolution SEM image of the obtained Ag nanowires, showing that the nanowires have round cross-sections with a regular polyhedron shape of Ag nanoparticles attached on the freestanding end. The length of the wires is up to 50 μm and the diameter is about 200 nm. The XRD pattern of the as-grown nanowires is depicted in Fig. 2(b), which identifies the resulting products as Ag nanowires. The nanowire ensembles are indexed perfectly to the face-centered cubic (fcc) crystal structure of Ag (JCPDS card no. 87-0717) with a lattice constant of a=4.085 Å.

Fig. 3(a) shows a TEM image of a typical silver nanowire. Fig. 3(b)～(d) presents selected area electron diffraction (SAED) patterns of the Ag nanowire shown in Fig. 3(a), which were taken at various locations separated by several

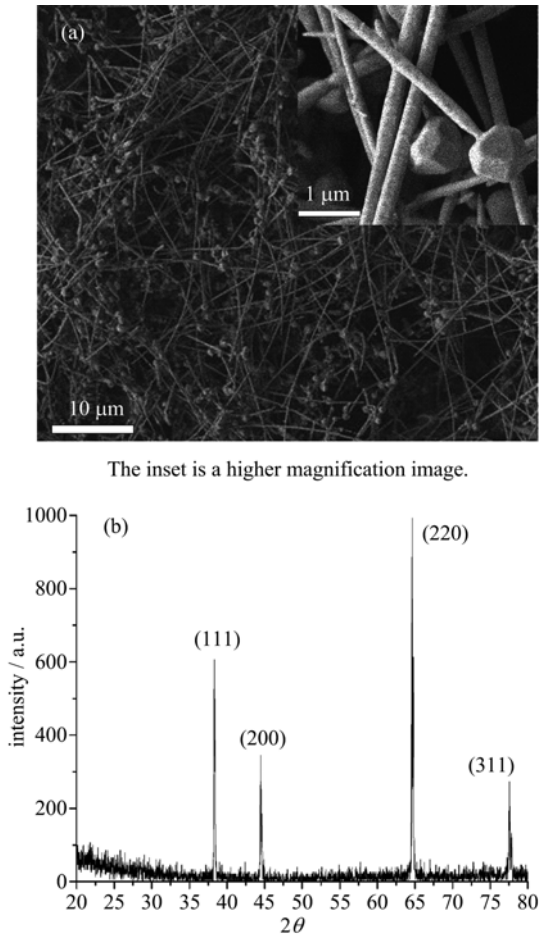

The inset is a higher magnification image.

Fig. 2 SEM image of the as-synthesized Ag nanowires (a), and typical XRD pattern of Ag nanowires (b)

micrometers. All of the spot patterns can be completely assigned to the same fcc Ag structure, further confirming the single-crystallinity of the whole nanowire. This also shows that the nanowires grow along the $[1\,\bar{3}1]$ crystallographic direction.

The diameters of the Ag nanowires could be

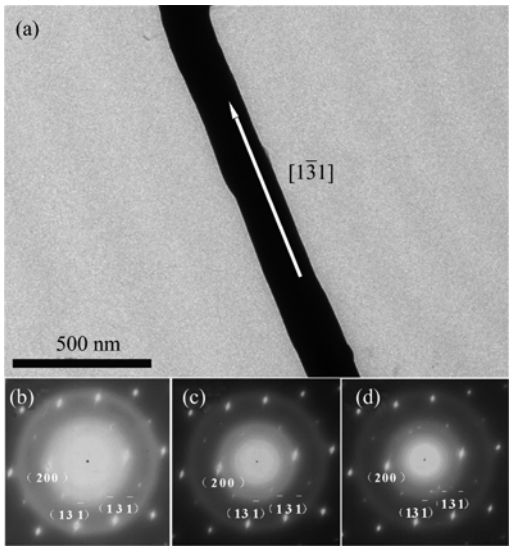

(a) TEM image of a Ag nanowire.
(b)～(d) SAED patterns taken at various regions of the Ag nanowire in (a)

Fig. 3　TEM image and SAED patterns of a Ag nanowire

modulated by changing the amount of $AgNO_3$ in the source. The lower Ag concentration in the vapor results in smaller alloy particles formed at the initial growth stage. According to the VLS mechanism, smaller catalyst particles lead to the decrease of the solid-liquid interface, so the central region of the interface is easier to be oxidized to form ZnO if the oxygen concentration remains the same. Thus, the diameters of the nanocable and the core will decrease as the amount of $AgNO_3$ decreases. Fig. 4(a) exhibits the SEM image of the nanocables grown with reduced amount of $AgNO_3$ of 0.25 g, but the same amount of ZnO. Fig. 4(b) shows the SEM image of an Ag nanowire obtained by etching the nanocables used for Fig. 4(a). It is clear that the diameter of the Ag core decreased from 200 nm for nanowires grown with $AgNO_3$ of 0.5 g (Fig. 2(a)), to 100 nm in average. The yield of Ag nanowires also reduced with the decrease in diameter.

The SERS sensitivity of these Ag nanowires was tested using Rhodamine B molecules. For comparison, Si and Ag film with a thickness of 100 nm coated on Si were used as reference samples. Fig. 5 shows the Raman spectra of 10^{-9} mol/L Rhodamine B molecules with the 514 nm excitation for Ag nanowiers, Si and Ag film, respectively. In comparison with the Si and Ag film, an obvious SERS effect is observed in the Ag nanowires and all the observed Raman bands agree well with the literature reports[27]. The Raman bands at about 1 363, 1 508, 1 559, and 1 648 cm^{-1} can be attributed to aromatic C—C stretching. The Raman bands at about 1 280 and 1 602 cm^{-1} can be attributed to C—C bridge-bands stretching and C=C stretching, respectively. No obvious variation in SERS enhancement was observed from one position to another in the same sample.

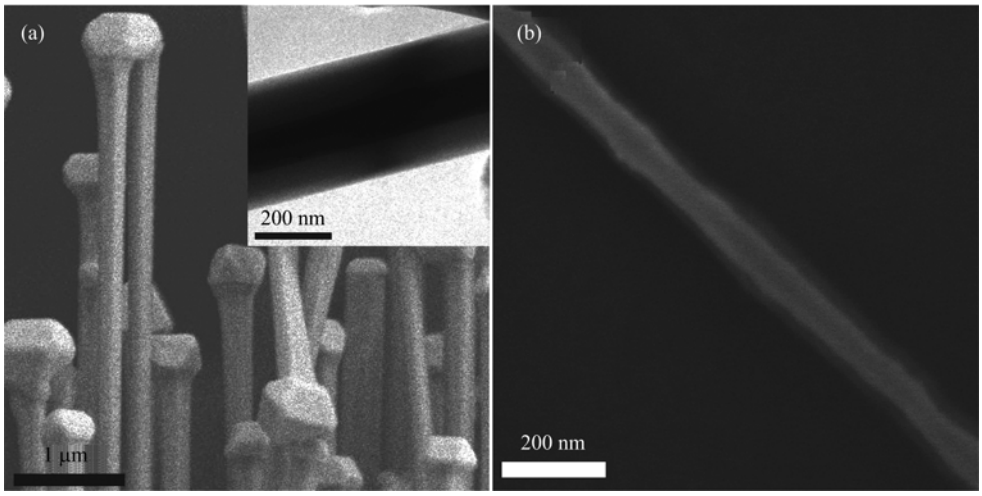

(a) SEM image of Ag/ZnO nanocables with $AgNO_3$ of 0.25 g. The inset in (a) is a TEM image.
(b) SEM image of an Ag nanowire etched from the Ag/ZnO nanocables in (a)

Fig. 4　SEM image of Ag/ZnO nanocables and Ag nanowire with $AgNO_3$ of 0.25 g

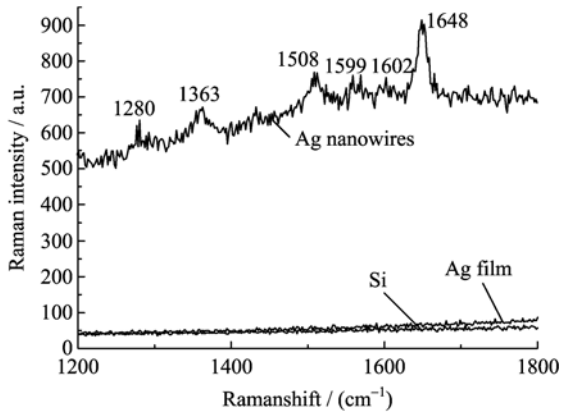

Fig. 5 Raman spectra of 1 nmol/L Rhodamine B molecules using Ag nanowires, Si and Ag film as substrates, respectively

3 Conclusion

High-yield and uniform Ag nanowires have been fabricated by thermal evaporation route via the VLS growth mechanism. The single-crystalline Ag nanowires have an fcc structure. The diameters can be modulated by changing the ratio of Ag in the source. SERS of Ag nanowires could reach the detection of 10^{-9} mol/L low concentration of Rhodamine B molecules.

References

[1] Jiang H L, Akita T, Ishida T, et al. Synergistic catalysis of Au@Ag Core-shell nanoparticles stabilized on metal-organic framework [J]. Journal of the American Chemical Society, 2011, 133: 1 304-1 306.

[2] Yin F, Lee S, Abdela A, et al. Communication: Suppression of sintering of size-selected Pd clusters under realistic reaction conditions for catalysis [J]. The Journal of Chemical Physics, 2011, 134: 141101.

[3] Conoci S, Petralia S, Samori P, et al. Optical transparent, ultrathin Pt films as versatile metal substrates for molecular optoelectronics [J]. Advanced Functional Materials, 2006, 16: 1 425-1 432.

[4] Chowdhury S, Bhethanabotla V R, Sen R. Effect of Ag-Cu alloy nanoparticle composition on luminescence enhancement/quenching [J]. The Journal of Chemical Physics C, 2009, 113: 13 016-13 022.

[5] Malinsky M D, Kelly K L, Schatz G C, et al. Chain length dependence and sensing capabilities of the localized surface plasmon resonance of silver nanoparticles chemically modified with alkanethiol self-assembled monolayers [J]. Journal of the American Chemical Society, 2001, 123: 1 471-1 482.

[6] Haes A J, Van Duyne R P. A nanoscale optical biosensor: Sensitivity and selectivity of an approach based on the localized surface plasmon resonance spectroscopy of triangular silver nanoparticles [J]. Journal of the American Chemical Society, 2002, 124: 10 596-10 604.

[7] Petty J T, Story S P, Juarez S, et al. Optical sensing by transforming chromophoric silver clusters in DNA nanoreactors [J]. Analytical Chemistry, 2012, 84: 356-364.

[8] Zhang X F, Kong X M, Fan W J, et al. Iminodiacetic acid-functionalized gold nanoparticles for optical sensing of myoglobin via Cu^{2+} coordination [J]. Langmuir, 2011, 27: 6 504-6 510.

[9] Hsiao W H, Chen H Y, Yang Y C, et al. Surface-enhanced Raman scattering imaging of a single molecule on urchin-like silver nanowires [J]. ACS Applied Materials & Interfaces, 2011, 3: 3 280-3 284.

[10] Xia X H, Zeng J, McDearmon B, et al. Silver nanocrystals with concave surfaces and their optical and surface-enhanced Raman scattering properties [J]. Angewandte Chemie International Edition, 2011, 50: 12 542-12 546.

[11] Wang Y L, Camargo P H C, Skrabalak S E, et al. A facile, water-based synthesis of highly branched nanostructures of silver [J]. Langmuir, 2008, 24: 12 042-12 046.

[12] Oliveira C C S, Ando R A, Camargo P H C. Size-controlled synthesis of silver micro/nanowires as enabled by HCL oxidative etching [J]. Physical Chemistry Chemical Physics, 2013, 15: 1 887-1 893.

[13] Liu S P, Chen N, Li L X, et al. Fabrication of Ag/Au core/shell nanowire as a SERS substrate [J]. Optical Materials, 2013, 35: 690-692.

[14] Liu S, Yue J, Gedanken A. Synthesis of long silver nanowires from AgBr nanocrystals [J]. Advanced Materials, 2001, 13: 656-658.

[15] You T, Xu S L, Sun S X, et al. Controllable synthesis of pentagonal silver nanowires via a simple alcohol-thermal method [J]. Materials Letters, 2009, 63: 920-922.

[16] Li W Z, Wei W, Chen J Y, et al. Stirring-assisted assembly of nanowores at liquid-solid interfaces [J]. Nanotechnology, 2013, 24: 105302.

[17] Sun Y G, Xia Y N. Large-scale synthesis of uniform silver nanowires through a soft, self-seeding, polyol process [J]. Advanced Materials, 2002, 14: 833-837.

[18] Bhattacharya B, Biswas J. Role of spacer lengths of

gemini surfactants in the synthesis of silver nanorods in micellar media [J]. Nanoscale, 2011, 3: 2 924-2 930.
[19] Kvítek L, Panáček A, Soukupová J, et al. Effect of surfactants and polymers on stability and antibacterial activity of silver nanoparticles (NPs) [J]. Journal of Chemical Physics C, 2008, 112: 5 825-5 834.
[20] Im H, Lee S H, Wittenberg N J, et al. Template-stripped smooth Ag nanohole arrays with silica shells for surface plasmon resonance biosensing [J]. ACS Nano, 2011, 5: 6 244-6 253.
[21] Zhang X L, Yu M, Liu J H, et al. Fabrication and characterization of Ag nanoparticles based on plasmid DNA as templates [J]. Materials Letters, 2011, 65: 719-721.
[22] Zeng J, Zheng Y Q, Rycenga M, et al. Controlling the shapes of silver nanocrystals with different capping agents [J]. Journal of the American Chemical Society, 2010, 132: 8 552-8 553.
[23] Morones J R, Frey W. Environmentally sensitive silver nanoparticles of controlled size synthesized with PNIPAM as a nucleating and capping agent [J]. Langmuir, 2007, 23: 8 180-8 186.
[24] Mohanty P, Yoon I, Kang T, et al. Simple vapor-phase synthesis of single-crystalline Ag nanowires and single-nanowire surface-enhanced Raman scattering [J]. Journal of the American Chemical Society, 2007, 129: 9 576-9 577.
[25] Chen C L, Furusho H, Mori H, et al. Silver nanowires with a monoclinic structure fabricated by a thermal evaporation method [J]. Nanotechnology, 2009, 20: 405605.
[26] Li Z, Wang G Z, Yang Q H, et al. Synthesis and electrical property of metal/ZnO coaxial nanocables [J]. Nanoscale Research Letters, 2012, 7: 316.
[27] Zhang J T, Li X L, Sun X M, et al. Surface enhanced Raman scattering effects of silver colloids with different shapes [J]. Journal of Chemical Physics B, 2005, 109: 12 544-12 548.

(上接第 95 页)

Remark 2.4 ① Ref. [3] constructed a system (X, T) such that $(K(X), T_K)$ is exactly Devaney chaotic, while the set of periodic points $Per(X, T)$ is nowhere dense. But this system does have periodic points.

② Ref. [8] constructed an HY-system (X, T) without periodic points. Then $(K(X), T_K)$ is Devaney chaotic, while the set of periodic points $Per(X, T)$ is empty.

Acknowledgement The authors wish to thank Wen Huang and Dominik Kwietniak for their careful reading and helpful suggestions.

References

[1] Bauer W, Sigmund K. Topological dynamics of transformations induced on the space of probability measures[J]. Monatsh Math, 1975, 79(2): 81-92.
[2] Banks J. Chaos for induced hyperspace maps [J]. Chaos Solitons Fractals, 2005, 25(3):681-685.
[3] Guirao J L G, Kwietniak D, Lampart M, et al. Chaos on hyperspaces [J]. Nonlinear Analysis: Theory, Methods & Applications, 2009, 71:1-8.
[4] Román-Flores H. A note on transitivity in set-valued discrete systems[J]. Chaos Solitons Fractals, 2003, 17(1): 99-104.
[5] Devaney R. An Introduction to Chaotic Dynamical Systems[M]. 2nd ed. Cambridge, MA: Westview Press, 2003.
[6] Banks J, Brooks J, Cairns G, et al. On Devaney's definition of chaos[J]. Amer Math Monthly, 1992, 99(4): 332-334.
[7] Furstenberg H. Disjointness in ergodic theory, minimal sets, and a problem in Diophantine approximation[J]. Math Systems Theory, 1967, 1: 1-49.
[8] Huang W, Ye X. Dynamical systems disjoint from any minimal system[J]. Trans Amer Math Soc, 2005, 357 (2): 669-694.
[9] Li J. Transitive points via Furstenberg family[J]. Topology Appl, 2011,158(16):2 221-2 231.
[10] Nadler S B. Hyperspaces of sets: A text with research questions[M]. New York / Basel: Marcel Dekker, 1978.
[11] Kwietniak D, Misiurewicz M. Exact Devaney chaos and entropy [J]. Qualitative Theory Dyanmical Systems, 2005, 6: 169-179.